

Long-term coexistence between the macroalga *Caulerpa prolifera* and the seagrass *Cymodocea nodosa* in a Mediterranean lagoon

M.D. Belando^{a,c,*}, J. Bernardeau-Esteller^a, I. Paradinas^b, A. Ramos-Segura^a, R. García-Muñoz^a, P. García-Moreno^c, L. Marín-Guirao^a, Juan M. Ruiz^{a,*}

^a Seagrass Ecology Group, Oceanographic Center of Murcia, Spanish Institute of Oceanography, Spain

^b Scottish Oceans Institute, University of St Andrews, KY16 8LB, St Andrews, Fife, UK

^c Asociación de Naturalistas del Sureste, Spain

ARTICLE INFO

Keywords:

Seagrass-seaweed interactions
Macrophytes mapping
Mar menor
Coastal lagoon

ABSTRACT

The potential negative influence of the seaweed *Caulerpa prolifera* on the seagrass *Cymodocea nodosa* was explored in a Mediterranean coastal lagoon (Mar Menor, Spain) where the alga suddenly and rapidly spread four decades ago. An extensive field sampling was carried out across the lagoon to characterise the distribution and abundance of both macrophytes at different spatial scales, as well as sediment characteristics. Generalised linear and additive models were performed at the whole-lagoon scale, for deep and shallow bottoms, independently, to explore factors influencing *C. nodosa* distribution and abundance. A high-spatial-resolution macrophyte distribution map was also generated by integrating underwater imaging, direct visualisations and orthophotographs. This map showed that both macrophytes largely dominated the ecosystem but with opposing depth patterns of abundance that mainly reflected their specific light requirements. *C. nodosa* was dominant at shallow depths but also grew intermingled with a dense *C. prolifera* bed over large areas of the deep seafloor with highly anoxic muddy sediments. Models did not reveal overall negative relationships between the macrophytes, indicating that *C. prolifera* was not the main driver of *C. nodosa* distribution and abundance in this coastal lagoon. Findings highlighted the absence of a negative direct or indirect influence of *C. prolifera* on *C. nodosa*, as supported by the fact that the distributions of both macrophytes were similar to those reported in the 1980s, just a few years after *C. prolifera* had spread in the lagoon. We conclude, therefore, that *C. prolifera* is not progressively replacing *C. nodosa* in this ecosystem, where both species have coexisted for decades.

1. Introduction

Primary production in non-eutrophic estuaries and coastal lagoons is essentially dominated by benthic vegetation, typically seagrass meadows (McGlathery et al., 2007). These meadows are recognised as one of the most valuable ecosystems on our planet because of the numerous ecosystem functions and services they provide (Costanza et al., 2014). These include, among others, control of coastal water quality through nutrient recycling, sediment stabilisation, pathogen removal and oxygen production (Costanza et al., 1997; Nordlund et al., 2016; Lamb et al., 2017). By acting as nutrient filters and sinks of particulate matter, seagrasses play a key role in protecting coastal lagoons and estuaries against eutrophication (McGlathery et al., 2007). Seagrass populations are, however, declining worldwide as a direct or indirect result of human activities and climate change, especially in coastal

lagoons and estuaries (McGlathery et al., 2007; Short et al., 2014; Pasqualini et al., 2017). These transitional (semi-)enclosed water bodies are subjected to increasing human pressures that commonly lead to eutrophication processes and the subsequent loss of benthic vegetation (Valiela et al., 1997), a situation that is expected to be aggravated as a result of the ongoing climate change (Lloret et al., 2008).

Seaweeds have increasingly been the cause of seagrass loss in coastal lagoons and estuaries, particularly when invasive seaweed species are involved and/or the system is subjected to nutrient enrichment (McGlathery, 2001; Burkepille and Hay, 2006; Holmer et al., 2011). Algal overgrowth can drastically impact seagrass populations via direct competition for light and by favouring anoxic conditions in both sediments and the canopy water column (Martínez-Lüscher and Holmer, 2010; Tamburello et al., 2014; Lanari et al., 2018). Compared to drifting/floating algae, the potential of rhizophytic algae to outcompete and

* Corresponding authors at: Seagrass Ecology Group, Oceanographic Center of Murcia, Spanish Institute of Oceanography, Spain.

E-mail addresses: mdolores.belando@ieo.es (M.D. Belando), juanm.ruiz@ieo.es (J.M. Ruiz).

replace local seagrasses is much lower, even if this group embraces species of the genus *Caulerpa*, a documented macroalgal invader of seagrass beds (Williams and Smith, 2007; Thomsen et al., 2012).

The *Caulerpa* species, including *C. prolifera* and highly invasive *C. cylindracea* and *C. taxifolia*, are capable of spreading rapidly over large areas of the seafloor and of creating dense mats on both soft and hard substrata, and also within seagrass beds (Klein and Verlaque, 2008; Glasby, 2013; Fabbri et al., 2015). The ability to modify the environment (e.g., underwater light, sediment redox) is considered one of the major mechanisms behind the displacement of seagrasses by *Caulerpa* species. The presence of dense *Caulerpa* stands increases sediment siltation and organic matter enrichment, which leads to reduced/anoxic conditions and the accumulation of phytotoxins in the sediment and water column (e.g., sulphides; Klein and Verlaque, 2008). Under such conditions, sulphide intrusion and toxicity are likely to occur in seagrasses, with the potential to increase plant mortality (Garcias-Bonet et al., 2008; Holmer and Hasler-Sheetal, 2014). Allelopathy may also favour the colonisation success of the genus *Caulerpa*, whose species produce and accumulate toxic allelochemicals in their tissues (e.g., caulerpenine; Paul and Fenical, 1987). The likely occurrence of allelopathic interactions between *Caulerpa* species and seagrasses derives from descriptive studies of naturally invaded populations but, to date, no experimental evidence for such negative interplay exists (De Villele and Verlaque, 1995; Dumay et al., 2002; Williams and Grosholz, 2002; Pergent et al., 2008). Competition for light could be another factor that underlies the replacement of seagrasses following *Caulerpa* invasion. As far as we know, however, there is no evidence that *Caulerpa* species compete effectively for light with seagrasses, at least for medium- and large-sized seagrass species (e.g., Raniello et al., 2004; Bernardeau-Esteller et al., 2015; Marín-Guirao et al., 2015).

Despite the numerous direct and indirect competitive interactions potentially involved in the substitution of seagrasses by *Caulerpa* seaweeds, experimental studies on the topic have provided inconclusive results and have not been able to demonstrate the role of *Caulerpa* species as drivers of seagrass loss (e.g., Ceccherelli and Sechi, 2002; Taplin et al., 2005; Glasby, 2013; Tuya et al., 2013; Bernardeau-Esteller et al., 2020). Most studies have, indeed, been unable to discriminate whether the negative correlation between the abundance of both macrophytes was the result of either real competitive interaction or simply an opportunistic response of the seaweed to seagrass decline caused by other disturbances (Terrados and Ros, 1991; Stafford and Bell, 2006; Lloret et al., 2008; Holmer et al., 2009; Höffle et al., 2011). Moreover, the time frame of these studies could also have affected our interpretations of algae–seagrass interactions because these interactions may change with time. By way of example, the effects of *C. taxifolia* on the seagrass *Cymodocea nodosa* can be severe in the short term (Ceccherelli and Cinelli, 1997), but harmless in the long term (Ceccherelli and Sechi, 2002). The final outcome of the interaction between *Caulerpa* species and seagrasses depends not only on the biological characteristics of the species involved (e.g., size; Thomsen et al., 2012), but also on the system's trophic status and nutrient dynamics (Davis and Fourqurean, 2001; Alexandre et al., 2017). All the above reasons imply that each system can respond differently to such biotic interactions, which hinders our ability to predict their long-term effect and hampers the conservation of coastal ecosystems under increasing seagrass stress from *Caulerpa* species.

The Mar Menor, one of the largest coastal lagoons of the Mediterranean Sea (135 km²), offers a valuable opportunity to explore long-term seagrass–seaweed interactions. The lagoon seafloor was colonised mainly by the seagrass *C. nodosa* (Ucria) Ascherson until the mid-1970s, when *C. prolifera* (Forsskål) J.V. Lamouroux entered the lagoon as a result of salinity reduction caused by the widening of the main channel that connects the lagoon with the adjacent Mediterranean Sea (Terrados, 1991). For the last four decades, the lagoon waters have experienced a relative increase in nutrient and chlorophyll concentrations due to the raising influx of nutrients from surrounding agricultural

areas (Velasco et al., 2006), with the potential to modify further the distribution of both benthic macrophytes. Previous studies on the distributions of benthic macrophytes in the Mar Menor have assumed a progressive decline of *C. nodosa* meadows concurrently with the expansion of *C. prolifera* in the ecosystem. Some authors have pointed out the potential negative effect of *C. prolifera* over *C. nodosa* as the likely explanation for the presumed seagrass regression (Pérez-Ruzafa et al., 1989; Pérez-Ruzafa et al., 2012), while others have suggested that the increased nutrient and particulate inputs into the lagoon were the main causes of this decline (Terrados and Ros, 1991; Lloret et al., 2005). These descriptive studies, however, were based on low spatial resolution samplings, lacking therefore a global integrated view of the heterogeneous conditions existing in the lagoon. In fact, the distribution of macrophytes in this lagoon has not been mapped in detail in recent decades, further limiting our understanding of the consequences of the long-term interaction between both macrophytes in the ecosystem.

In the present study, we aimed to determine whether *C. prolifera* is the major driver of the distribution and abundance patterns of *C. nodosa* in the Mar Menor coastal lagoon. For this purpose, an extensive sampling was conducted across all the lagoon to characterise the abundance of both macrophytes in terms of biomass, cover and shoot density, and the physico-chemical characteristics of the sediment (i.e., organic matter content, granulometry and depth). The information derived from this benthic sampling was integrated with towed underwater camera recordings, direct visualisations and orthophotographs to generate a detailed mapping of macrophyte distribution in the lagoon. In addition, through generalised additive models (GAMs), we investigated the likely existence of interactions between *C. nodosa* and *C. prolifera*, sediment characteristics and depth. We hypothesise that if *C. prolifera* has strongly and negatively influenced the distribution and abundance of *C. nodosa* during the last decades, the presence of the seagrass should be currently restricted to areas with low or no presence of the seaweed and that GAM models should display negative relationships between the abundance of both macrophytes.

2. Material and methods

2.1. Study site

The Mar Menor is one of the largest coastal lagoons (135 km²) on the Mediterranean coastline, with an average depth of 3.7 m and maximum depth of 7 m in the central lagoon areas (Fig. 1). The system is isolated from the Mediterranean Sea by a sandy bar 22 km long and interrupted by only five shallow channels through which seawater exchanges. The salinity in the 1960s was higher than it currently is (maximum of 53 vs. 47; Navarro, 1927; Más-Hernandez, 1996), when *C. nodosa* and *Ruppia cirrhosa* were already present in the lagoon (Navarro, 1927; Lozano Cabo, 1954). The widening of the El Estacio inlet in 1973 further reduced salinity and favoured the introduction and spreading of *C. prolifera* in the lagoon (Ballester, 1985; Terrados and Ros, 1991). Since then, *C. nodosa* and *C. prolifera* have dominated the lagoon seafloor, despite receiving increasing nutrient inputs from surrounding agricultural areas (Terrados and Ros, 1991; Pérez-Ruzafa et al., 2002; Velasco et al., 2006). Therefore, the Mar Menor lagoon has historically been considered a hypersaline–oligotrophic macrophyte-dominated system, with benthic primary production dominating over planktonic production (Terrados and Ros, 1991).

2.2. Characterisation of benthic vegetation and sediments

The field sampling was carried out in early summer (July) of 2014, corresponding to the seasonal peak development of both macrophytes in the coastal lagoon (Ballester, 1985; Terrados and Ros, 1991). A total of 49 sampling points, distributed over the lagoon seabed as uniformly as possible, were sampled to characterise the abundance of *C. nodosa* and *C. prolifera* together with sediment characteristics. This sampling point

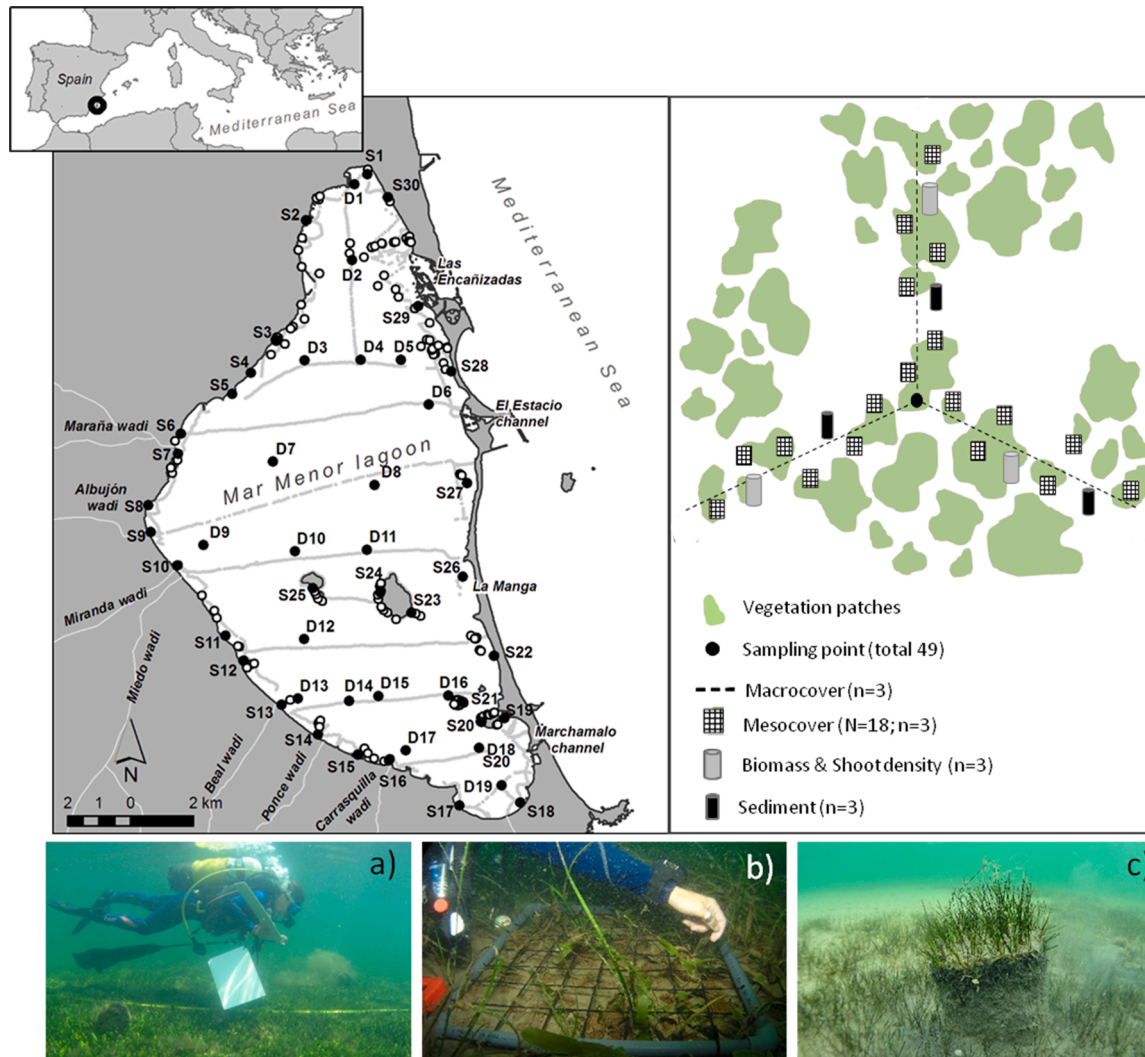


Fig. 1. Map of the Mar Menor lagoon and schematic representation of the sampling design. Grey lines indicate the trajectory followed by the video camera. Black circles correspond to the 49 sampling sites. Empty circles denote visual observations. a) estimation of macrophyte macrocover along a 50-m long linear transect, b) mesocover estimation on a 50 × 50 cm quadrat, and c) core sample collection for the determination of macrophytes biomass and *C. nodosa* shoot density.

network incorporated 20 points that had been included in previous studies (e.g., Ballester, 1985) and 29 additional points that were selected to expand and complete our sampling, especially in shallow areas (<3 m depth) where the habitat is more heterogeneous. At each sampling point, *C. nodosa* and *C. prolifera* abundance was properly characterised on the different hierarchical scales at which the meadow structure is organised (Robbins and Bell, 1994; Vidondo et al., 1997). Specifically, patch scale (i.e. small vegetation patches primarily formed by macrophytes), mesoscale (i.e. large vegetation patches emerging from the aggregation of smaller patches) and macroscale (or landscape scale i.e. the landscape formed by larger patches). Shoot density (only for *C. nodosa*) and biomass were determined at the patch scale and the percentage cover on both meso and macro-scales (mesocover and macrocover, respectively).

Fig. 1 shows a schematic representation of the sampling design. At each sampling point, three 50-m long linear transects were established at fixed angles (0, 120 and 240°) to measure the different metrics ($n = 3$). *C. nodosa* and *C. prolifera* macrocovers ($MCy = C. nodosa$, $MCAu = C. prolifera$) were determined as the total length of the transect with a presence of each species. In addition, macrophyte cover on the meso-scale (where mCy and $mCau$ are the mesocovers of *C. nodosa* and *C. prolifera*, respectively) was estimated on six 50 × 50 cm quadrats allocated randomly within large patches along each of the three linear transects and averaged for each transect. These quadrats were

subdivided into 60 subquadrats and the abundance of each species estimated as the percentage of subquadrats that they occupied. On the patch scale level, the biomass of both macrophytes ($BCy = C. nodosa$ biomass, $BCau = C. prolifera$ biomass), and the shoot density of *C. nodosa* (DCy) were determined from three core samples (15-cm diameter) collected at each sampling point (one sample within small patches for all three linear transects). Samples were transported to the laboratory in coolers, where *C. nodosa* leaves, sheaths, rhizomes and roots and *C. prolifera* fronds and stolons were carefully separated, cleaned of sediment and epiphytes and dried to constant weight (60 °C for 24–48 h) to determine their biomass as dry weight (DW). Shoot density (shoots m^{-2}) was obtained from the total number *C. nodosa* shoots contained in all three cores.

Three sediment samples were also collected by divers at each sampling point by using cores (7-cm diameter). Sediment grain size was analysed by dry sieving, following Kramer (1987). Briefly, sediments were treated with H_2O_2 (24 h) and then washed and centrifuged to remove salts and organic matter. Washed sediments were then treated with sodium-hexametaphosphate and Na_2CO_3 solution and stirred for 2 h to disperse clusters. Subsequently, samples were oven-dried (24–48 h at 105 °C) and sieved through a stacked set of graded sieves in the 2000–63 μm range (coarse sand = 2 mm – 200 μm (CSand); fine sand = 200–0.063 μm (FSand); and silt-clay fraction <0.063 μm (SiltClay). The

sediment organic matter content (OM) was determined as the percentage of weight loss upon calcining dry sediment in a muffle furnace at 550 °C for 5 h.

2.3. Mapping benthic vegetation

A macrophyte distribution map was generated from 189 direct visual observations from a boat or by diving (Fig. 1). These observations were complemented by the 49 sampling points and with the georeferenced recordings obtained by video camera trawled along 155.5 km of continuous recording (Fig. 1). The video camera was mounted on a structure and towed over the seafloor at a fixed distance of ca. 150 cm. Depth was measured continuously during recordings (Echotest II, France). The characterisation of shallow areas was complemented with a series of orthoimages from the Spanish National Geographical Institute (PNOA 2013 ©), which were validated *in situ* by direct observations. The benthic vegetation distribution map was created using the ArcGIS 10.2® software (ESRI®).

2.4. Data analysis

All parameters were initially screened based on their Pearson correlation coefficients (see supplementary Tables S1, S2 and S3). When two predictor variables showed correlation coefficients greater than 0.6, they were not included in the same model to reduce multicollinearity, but independent models including each of them were built for their subsequent comparison during model selection.

We applied generalised additive models (GAMs) to analyse the linear and nonlinear relationships between each of the *C. nodosa* descriptors (MCy, mCy, BCy and DCy) and *C. prolifera* abundance (MCau, mCau and BCau), sediment characteristics (CSand, FSand, SiltClay and OM) and depth (D), as predictor variables. Each of the four *C. nodosa* descriptors were analysed at the global scale (N = 49) and for shallow (<3 m, N = 30) and deep (>3 m, N = 19) bottoms independently. In these analysis, the biomass and shoot density of *C. nodosa* were log-transformed to approximate normality, while the macro- and mesocover were analysed through beta regression. Beta distribution constitutes an appropriate method for modelling rates and proportions within the standard unit interval (0–1) (Ferrari and Cribari-Neto, 2004).

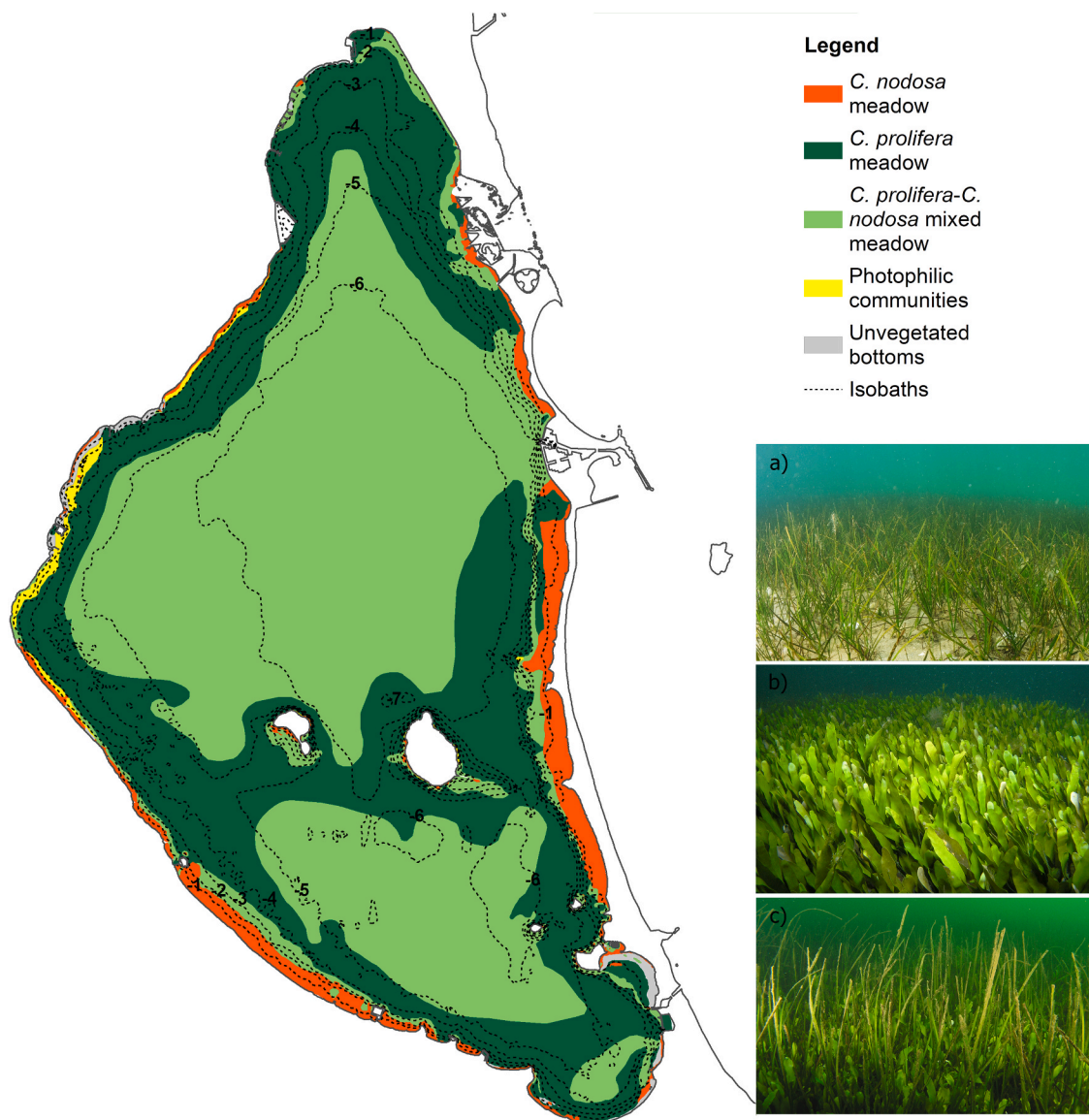


Fig. 2. Benthic macrophyte distribution in the Mar Menor lagoon in 2014: a) *C. nodosa* meadows; b) *C. prolifera* beds; c) deep *C. nodosa* and *C. prolifera* mixed meadows. The dashed lines indicate depth isobaths with a contour interval of 1 m.

A set of models were built for each of the four *C. nodosa* descriptors, each set including the individual effect of all studied predictors variables, the potential interactions of each *Caulerpa* descriptor with the different sediment fractions (CSand, FSand, SiltClay), OM and D, as well as other potential interactions with ecological relevance, e.g. SiltClay vs OM.

The final models were selected based on the corrected Akaike's Information Criterion for small samples (AICc), and models with an AICc difference of less than two points were considered as alternative models.

3. Results

3.1. Spatial distribution and abundance of *C. nodosa* and *C. prolifera* in the lagoon

In all, 13,166 ha of lagoon bottom was colonised by the two

dominant macrophytes *C. nodosa* and *C. prolifera*, and only a small fraction of the bottom was unvegetated (i.e., 161 ha; Fig. 2). A detailed high-resolution map is available at <https://github.com/GEAM-IEO/Mar-Menor-lagoon-2014>. *C. nodosa* was distributed over 8052 ha and formed monospecific meadows only in the shallower areas of the lagoon (<2 m depth). The species also formed mixed meadows with *C. prolifera* at shallow depths but mainly in deep bottoms (>4 m depth).

C. nodosa occupied a large proportion of the seabed (macro- and mesocover >50 %; Fig. 3, Fig. S1), although the macrocover and mesocover values were higher on shallow bottoms (67.4 ± 23.6 % and 83.4 ± 19.0 %, respectively) than in deep waters (47.1 ± 26.4 % and 38.7 ± 16.2 %, respectively; average \pm SD). Despite occupying a high percentage of the lagoon floor irrespective of depth, the abundance of this species in biomass and shoot density terms was markedly higher in shallow than in deep lagoon areas (Fig. S1). Accordingly, *C. nodosa* biomass and shoot density were (average \pm SD) 1032 ± 407 g DW m⁻²

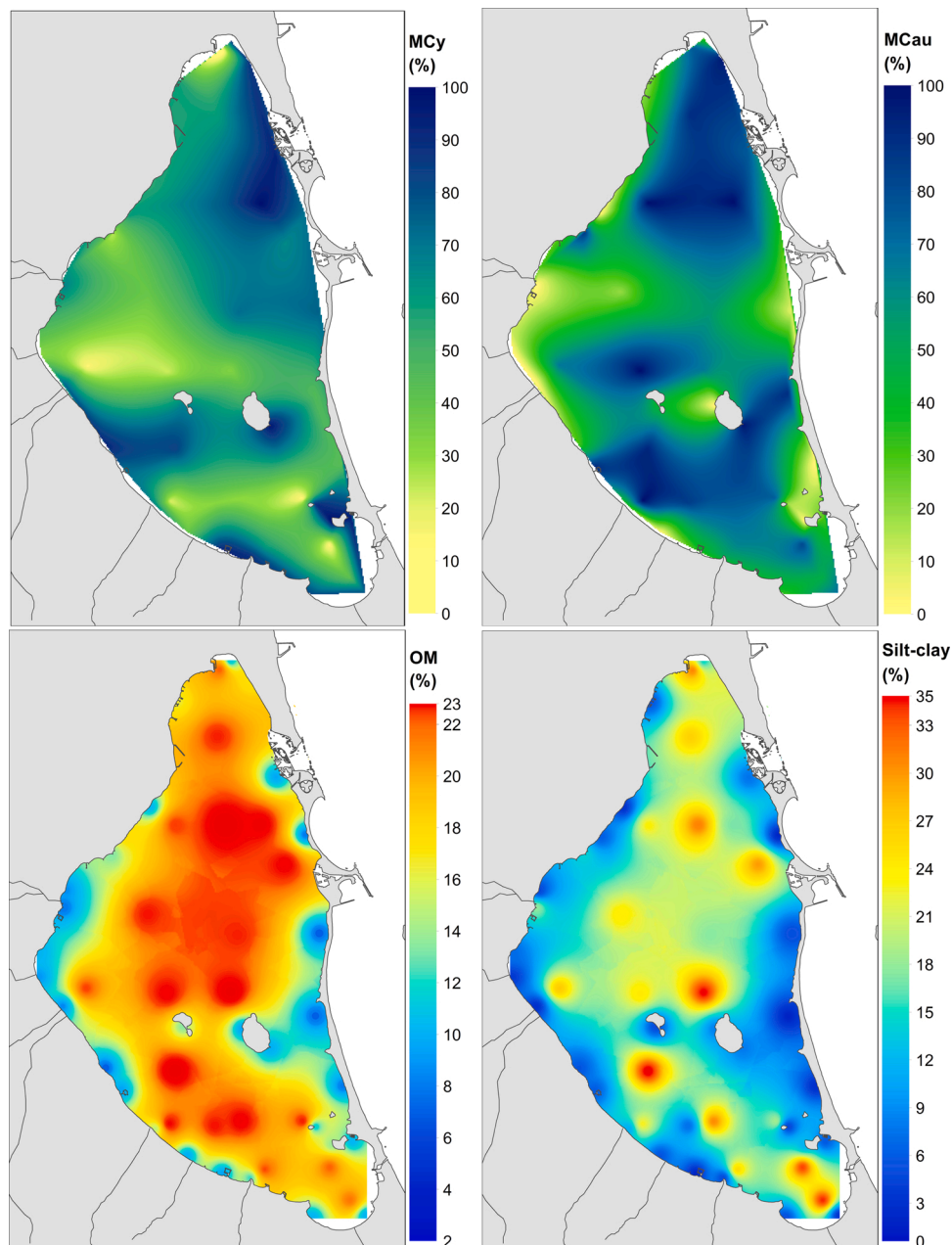


Fig. 3. Spatial variations of *C. nodosa* and *C. prolifera* macrocover (MCy, MCau), organic matter (OM) and silt-clay content in sediments from the Mar Menor coastal lagoon in 2014.

and 3995 ± 1529 shoots m^{-2} in shallow waters, and 182 ± 128 g DW m^{-2} and 1050 ± 348 shoots m^{-2} in deep waters.

C. prolifera occupied a total area of 12,530 ha of the lagoon floor (94 %; Fig. 2). The species formed monospecific beds between 2 and 4 m depth and was barely present at shallower depths (<1–2 m). *C. prolifera* macro- and mesocover showed a similar spatial pattern over the entire lagoon (Fig. 3, Fig S2), with higher values prevailing at greater depths (>4 m). Average percentages of the macro- and mesocover on deep bottoms were 76.6 ± 21.7 % and 61.7 ± 34.2 % (average \pm SD), respectively, while the corresponding values on shallow bottoms were 36.0 ± 33.0 % and 19.9 ± 29.2 %. *C. prolifera* biomass was also higher at greatest depths, where almost 70 % of the sampled points had biomass values well above 100 g DW m^{-2} . Conversely, the vast majority of the shallow sampling points (80 %) had biomass levels below 50 g DW m^{-2} . The angiosperm *Ruppia cirrhosa* was also observed growing in a few particular localities of the northeast coastline of the lagoon (see <https://github.com/GEAM-IEO/Mar-Menor-lagoon-2014>). It covered a total of 70 ha on shallow bottoms and formed small monospecific and mixed meadows together with *C. nodosa* and *C. prolifera*.

Wide extensions of the deep lagoon sediments (>2 m depth) were characterised by a high proportion of fines (silt–clay) and OM (Fig. 3), whereas the sediments on shallow bottoms (<2 m depth) showed that sands and lower OM content predominated (Fig. 3, Fig. S3). The silt–clay content was (average \pm SD) 24.3 ± 7.7 % and 5.9 ± 6.4 % in deep and shallow sediments, respectively, while the corresponding levels of OM content were 18.1 ± 2.2 % and 4.2 ± 2.9 %.

3.2. Relationship of *C. nodosa* descriptors with *C. prolifera* and sediment characteristics

Correlation analyses showed significant positive correlations between the response variables DCy and BCy at the whole lagoon (Table S1) and the deep seabed scale (Table S3). Regarding the predictors, all *C. prolifera* abundance variables (MCau, mCau and BCau) were always positively correlated with each other (Tables S1, S2 and S3). The organic matter content (OM) was highly and positively correlated with depth (D) and silt-clay fraction (SiltClay) at the whole-lagoon scale (Table S1). The CSand fraction was negatively correlated with FSand at the global scale and on shallow bottoms (Tables S1 and S2) and with SiltClay on deep bottoms (Table S3).

At the whole-lagoon scale (shallow and deep sampling points), the best-fitting models for *C. nodosa* macrocover (MCy) and density (DCy) showed non-linear variations with D (Table 1). The abundance of the seagrass decreased with the increase in depth of shallow bottoms (until 3–3.5 m) but it increased or remained relatively stable at greater depths (Fig. 4a and d). Moreover, the alternative models of these seagrass descriptors (MCy and DCy) also revealed a differential relationship between the two macrophytes depending on depth (Tables S4 and S5, Fig. S4). Similarly, the best-fitting models for *C. nodosa* mesocover (mCy) and biomass (BCy) showed nonlinear relationships with the interaction of *C. prolifera* abundance and depth (Table 1, Fig. 4b and c). Since the influence of depth and OM cannot be dissociated, these results revealed that patterns of variations of the two macrophytes differed between shallow bottoms (<3 m) with a low OM content (<11 %) and deep bottoms (>3 m) with a higher OM content (14–23 %). Overall, these models showed a high percentage of explained deviance, indicating the prominent effect of depth on patterns of variations in *C. nodosa* abundance as well as on its relationship with *C. prolifera* in the lagoon (Table 1, Fig. 4).

Regarding shallow bottoms, the best-fitting models for MCy, mCy and BCy did not display any negative relationships with *C. prolifera* predictors (Table 1). The individual effect of *C. prolifera* and its interaction with OM or FSand was always positive. In fact, the highest values of these *C. nodosa* descriptors were found on bottoms with dense *C. prolifera* stands and high OM or FSand percentages (Fig. 5a, c and d). Only DCy showed a negative linear relationship with mCau and with

FSand (Table 1). It is noteworthy, however, that the percentage of explained deviance of all these models was relatively low (<40 %; Table 1), which suggests that the influence of studied predictors on *C. nodosa* abundance is limited on shallow bottoms of the lagoon.

With regard to deep bottoms, the best-fitting models selected OM and *C. prolifera* abundance (MCau, mCau) as significant predictors of the variability in *C. nodosa* abundance. The OM content in sediments had a linear and positive effect on *C. nodosa* at the macro and mesoscale level (MCy and mCy, Table 1), while the best-fitting models for BCy, DCy and mCy revealed a nonlinear relationship between the two macrophytes (Table 1, Fig. 6). This relationship was positive in the case of *C. nodosa* density and biomass (DCy and BCy), which was especially evident in highly abundant *C. prolifera* stands (MCau higher than 75 %) (Fig. 6b and c). At the patch level (mCy), a more complex pattern of variation was found in both species. In this case, the highest abundance of *C. nodosa* was observed on bottoms where *C. prolifera* mesocover was within the range of 30–70 %, while it showed minimum values outside this range. The interaction between *C. prolifera* abundance and OM was not retained as a significant predictor in any of the best-fitting models for deep bottoms, while the potential alternative models (e.g. at MCy and BCy level) even revealed a positive effect of this interaction on *C. nodosa* abundance (Tables 1, S4 and S5, Fig. S6). Results from deep-bottom models showed higher explained deviance than from shallow-bottom models, indicating a greater influence of the studied predictors on *C. nodosa* abundance across the deep seabed of the lagoon (Table 1).

4. Discussion

Our comprehensive study of benthic vegetation in the Mar Menor coastal lagoon did not support the existence of negative interactions between the seagrass *C. nodosa* and the seaweed *C. prolifera* in the ecosystem. The high-spatial-resolution map of benthic macrophyte distribution here outlined showed that *C. nodosa* and *C. prolifera* were the dominant macrophytes in the Mar Menor in 2014, after at least four decades of coexistence in the lagoon. In addition, GAM models did not reveal negative relationships between the abundance of both macrophytes but that these associations were complex and varied according to other predictor variables (e.g., depth). On the basis of these findings, we can assume that the distribution of *C. nodosa* has experienced little change since the establishment and spread of *C. prolifera*, and, thus that the presence of the chlorophyte was not the main driver of seagrass distribution and abundance in this coastal lagoon.

The seaweed *C. prolifera* was the most ubiquitous species in the Mar Menor and grew over almost the entire lagoon area. Its abundance showed a marked bathymetric pattern, with higher biomass values in deeper lagoon areas (>4 m depth), where the species formed an extensive dense bed. This distribution pattern is most likely related to the photo-physiology of the species, which suffers from photodamage in shallow waters and is more productive under dim light conditions in deeper areas (Terrados and Ros, 1992; García-Sánchez et al., 2012). For its part, the seagrass covered over 60 % of the lagoon floor and formed lush perennial monospecific meadows and mixed meadows with *C. prolifera* in shallow waters, as well as extensive mixed meadows across the deep lagoon seabed. In deep bottoms, despite the high abundance of *C. prolifera*, the relative area covered by the seagrass *C. nodosa* was also high (macro- and mesocovers of >50 %), frequently with values similar to those found in shallower depths. Even so, the abundance of *C. nodosa* also showed a marked bathymetric gradient but with an inverse pattern to that of *C. prolifera*, with the seagrass abundance (biomass and shoot density) decreasing from shallow to deep bottoms, although this most likely reflected the effect of light extinction along the water column rather than a negative interaction between the macrophytes, as discussed below. On the one hand, ‘canopy-opening’ to facilitate light penetration and ‘below-ground-mass-depletion’ to maintain plant carbon balances are well documented structural photo-acclimative responses of seagrass meadows to depth (e.g., Olesen et al., 2002; Collier

Table 1

Results of the best-fitting models conducted at the whole-lagoon scale (global analysis) and for shallow and deep bottoms independently. Response variables: *C. nodosa* macrocover (MCy), mesocover (mCy), biomass (BCy) and shoot density (DCy). Predictor variables: depth (D), *C. prolifera* macrocover (MCau), mesocover (mCau) and biomass (BCau), organic matter (OM), fine sand (FSand), coarse sand (CSand) and silt and clay content (SiltClay) in sediments. Dev.Expl. = deviance explained. For GAM models: the function *te* defines tensor product smoothing splines, and *s* indicates non-linear smoothing splines.

GLOBAL ANALYSIS: SHALLOW + DEEP BOTTOMS							
Best fitted model	Parametric coefficients:	Estimate	Std. Error	z/t value	Pr(> z /t)	R ² (adj)	Dev. Expl. (%)
<i>C. nodosa</i> macrocover (MCy)							
MCy ~ s(D)	Intercept	0.39	0.14	2.77	0.005	0.18	25
	<i>Smooth terms:</i>	<i>edf</i>	<i>Ref.df</i>	<i>Chi.sq</i>	<i>p-value</i>		
	D	2.42	2.77	9.28	0.013		
<i>C. nodosa</i> mesocover (mCy)							
mCy ~ te(D, MCau)	Intercept	0.87	0.11	7.61	<0.0001	0.75	78
	<i>Smooth terms:</i>	<i>edf</i>	<i>Ref.df</i>	<i>Chi.sq</i>	<i>p-value</i>		
	D x MCau	6.34	6.82	110.4	<0.0001		
<i>C. nodosa</i> biomass (BCy)							
log BCy ~ te(D, MCau)	Intercept	6.12	0.07	81.53	<0.0001	0.79	83
	<i>Smooth terms:</i>	<i>edf</i>	<i>Ref.df</i>	<i>F</i>	<i>p-value</i>		
	D x MCau	8.69	10.46	17.27	<0.0001		
<i>C. nodosa</i> shoot density (DCy)							
log DCy ~ s(D)	Intercept	7.71	0.05	132.9	<0.0001	0.73	74.7
	<i>Smooth terms:</i>	<i>edf</i>	<i>Ref.df</i>	<i>F</i>	<i>p-value</i>		
	D	2.51	2.83	46.04	<0.0001		
SHALLOW BOTTOMS							
Best fitted model	Parametric coefficients:	Estimate	Std. Error	z/t value	Pr(> z /t)	R ² (adj)	Dev. Expl. (%)
<i>C. nodosa</i> macrocover (MCy)							
MCy ~ BCau * FSand	Intercept	1.03	0.17	6.24	<0.0001	0.17	31
	FSand	-0.08	0.17	-0.45	0.650		
	BCau	0.53	0.24	2.19	0.028		
	BCau x FSand	0.63	0.22	2.9	0.004		
<i>C. nodosa</i> mesocover (mCy)							
mCy ~ SiltClay * OM + MCau * OM	Intercept	2.11	0.16	12.84	<0.0001	0.26	34
	SiltClay	-0.06	0.21	-0.32	0.745		
	MCau	0.26	0.17	1.57	0.116		
	OM	0.53	0.2	2.58	0.0099		
	OM x MCau	0.57	0.21	2.78	0.0054		
	OM x SiltClay	-0.62	0.17	-3.53	0.0004		
<i>C. nodosa</i> biomass (BCy)							
log BCy ~ CSand + SiltClay:OM + MCau * OM	Intercept	6.95	0.06	104.18	<0.0001	0.15	30
	OM	0.071	0.074	0.96	0.34		
	CSand	0.13	0.06	1.94	0.064		
	SiltClay x OM	-0.14	0.074	-1.94	0.064		
	MCau	0.15	0.072	2.09	0.047		
	MCau x OM	0.2	0.085	2.37	0.026		
<i>C. nodosa</i> shoot density (DCy)							
log DCy ~ FSand + mCau	Intercept	8.26	0.05	150.13	<0.0001	0.33	38
	FSand	-0.15	0.05	-2.58	0.016		
	mCau	-0.19	0.05	-3.47	0.0017		
DEEP BOTTOMS							
Best fitted model	Parametric coefficients:	Estimate	Std. Error	z/t value	Pr(> z /t)	R ² (adj)	Dev. Expl. (%)
<i>C. nodosa</i> macrocover (MCy)							
MCy ~ OM	Intercept	-0.18	0.23	-0.77	0.44	0.18	30.5
	OM	0.61	0.24	2.532	0.011		
<i>C. nodosa</i> mesocover (mCy)							
mCy ~ s(mCau) + OM	Intercept	-0.58	0.14	-4.051	<0.0001	0.41	60
	OM	0.54	0.17	3.13	0.0018		
	<i>Smooth terms:</i>	<i>edf</i>	<i>Ref.df</i>	<i>Chi.sq</i>	<i>p-value</i>		
	mCau	2.33	2.7	12.2	0.0049		
<i>C. nodosa</i> biomass (BCy)							
log BCy ~ s(MCau)	Intercept	4.88	0.1231	39.7	<0.0001	0.53	60
	<i>Smooth terms:</i>	<i>edf</i>	<i>Ref.df</i>	<i>F</i>	<i>p-value</i>		
	MCau	2.63	2.89	7.97	0.004		
<i>C. nodosa</i> shoot density (DCy)							
log DCy ~ s(MCau)	Intercept	6.84	0.07	89.45	<0.0001	0.42	53
	<i>Smooth terms:</i>	<i>edf</i>	<i>Ref.df</i>	<i>F</i>	<i>p-value</i>		
	MCau	2.83	3.33	4.018	0.033		

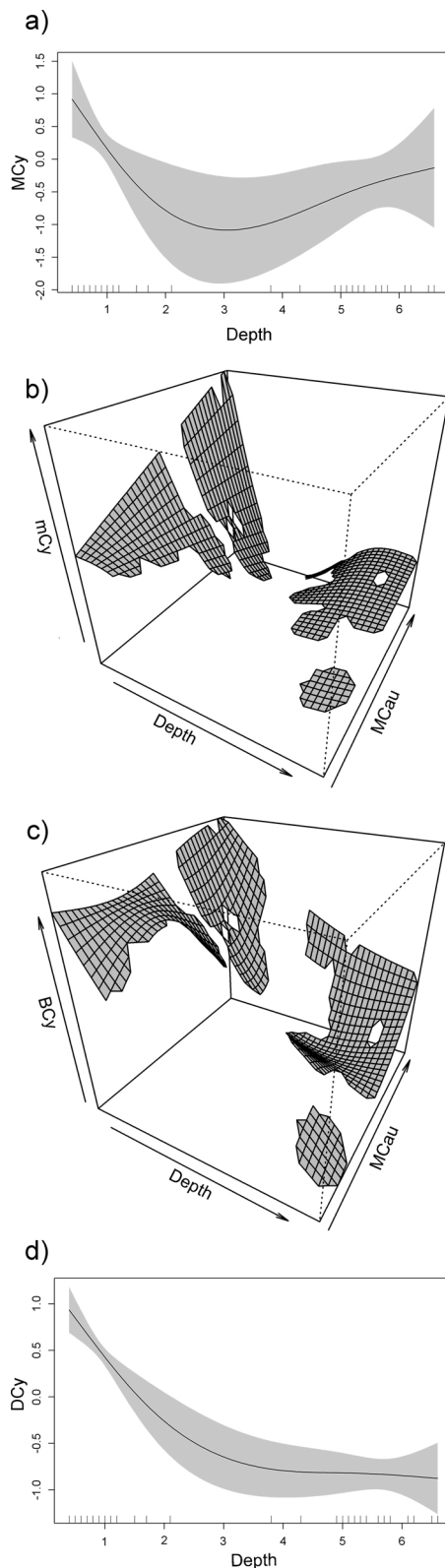


Fig. 4. Graphical representation derived from the best-fitting models conducted at the whole-lagoon scale showing the non-linear effect of depth on *C. nodosa* abundance (a,d), and the relationship of *C. nodosa* with the interaction of *C. prolifera* and depth (b,c). Response variables: *C. nodosa* macrocover (MCy), mesocover (mCy), biomass (BCy) and density (DCy). Predictors: *C. prolifera* macrocover (MCau) and depth.

et al., 2008; Enríquez et al., 2019). Therefore, the strong gradient of *C. nodosa* abundance in this shallow ecosystem is presumably reflecting the optical characteristics of the lagoon waters, which have become relatively turbid in recent decades (i.e., moderate peaks of light attenuation coefficient, $K_d = 0.2\text{--}0.5\text{ m}^{-1}$; Terrados, 1991; Lloret et al., 2005; Pérez-Ruzafa et al., 2019). This is in parallel with the spread of *C. prolifera* in the 1970s as a result of nutrient inputs from adjacent agricultural areas (Velasco et al., 2006; Martínez et al., 2007). In fact, similar abundance patterns have been described for the species in other shallow coastal ecosystems with similar water-column optical properties (e.g., Ebro Delta, $K_d = 0.38\text{--}0.57\text{ m}^{-1}$; Pérez and Romero, 1992; Olesen et al., 2002). On the other hand, statistical models did not identify *C. prolifera* abundance as a major factor determining the bathymetric pattern of *C. nodosa* abundance in the lagoon, but its interaction with depth. This complex nonlinear relationship indicated that the interaction between macrophytes varied according to depth, which prompted us to conduct independent analysis with shallow and deep datasets to remove the influence of depth from our analyses.

Shallow-bottom models showed that the pattern of *C. nodosa* distribution and abundance were poorly explained by predictor variables at shallow depths (30–38 % of deviance explained). These shallow areas are generally characterised by high environmental heterogeneity and by different degrees of human influence (e.g., recreational ports, beach nourishment, dredging, artificial rocky structures; Conesa et al., 2007). This involves a higher number of factors shaping the distribution and abundance of shallow macrophytes assemblages, as evidenced in relation to lagoon fish assemblages (Pérez-Ruzafa et al., 2006). Deep models, for their part, explained a higher proportion of the overall variability of *C. nodosa* abundance in the deep lagoon seabed (up to 68 % of deviance explained), in accordance with the more homogenous conditions existing in these large areas of the lagoon. The abundance of *C. prolifera* and the OM content in sediments were identified as the main explanatory variables for the patterns of *C. nodosa* abundance on the deep sea floor. Deep bottoms were muddy and contained high levels of OM, the highest in the whole lagoon, as a result of the major effect that dense *C. prolifera* may have on the organic enrichment of sediments (Holmer et al., 2009) given its high productivity rate and its relevant role as a particulate trap (Lloret and Marín, 2009; Hendriks et al., 2010). This, in turn, promotes highly reducing conditions and the build up of phytotoxic gases in sediments (Holmer et al., 2009), which did not apparently affect the capacity of *C. nodosa* to thrive and spread over large areas of the deep lagoon floor. *C. nodosa* is, indeed, one of the most tolerant seagrass species to such extreme sediment anoxic conditions (Terrados et al., 1999), which is congruent with the positive relationship found between its abundance (at macrocover, shoot density and biomass scale) and OM or *C. prolifera* abundance (Table 1). This is consistent with previous studies that reported extensive vegetative development of this seagrass species in highly anoxic muddy sediments in the studied lagoon (Terrados and Ros, 1992) and in other similar ecosystems (Perez et al., 1994), but is contrary to what might be expected if the seaweed had a negative influence on the seagrass in the lagoon. Only at the mesocover scale (i.e., patch level) was the relationship between the two macrophytes fairly complex, as shown by the model-derived bell-shaped abundance curve. The seagrass mesocover appeared to be independent from *C. prolifera* abundance in mixed meadows with intermediate values of algal abundance (from 30 % to 70 %), where the seagrass was present at the highest levels. Above this range of *C. prolifera* abundance (>70 %) the mesocover of the seagrass was lower, which could be interpreted as indicating a negative relationship between the two species. This contrast with the positive relationship mentioned above for *C. nodosa* biomass and density, which are seagrass descriptors, that should also reflect the presumable negative relationship between the two species. Moreover, low values of seagrass mesocover were also found when the abundance of the algae was low (<30 %). Since sparse *C. nodosa* patches were found across the deep bottoms irrespectively of whether the algae was abundant or scarce, other local factors could be influencing the patterns of

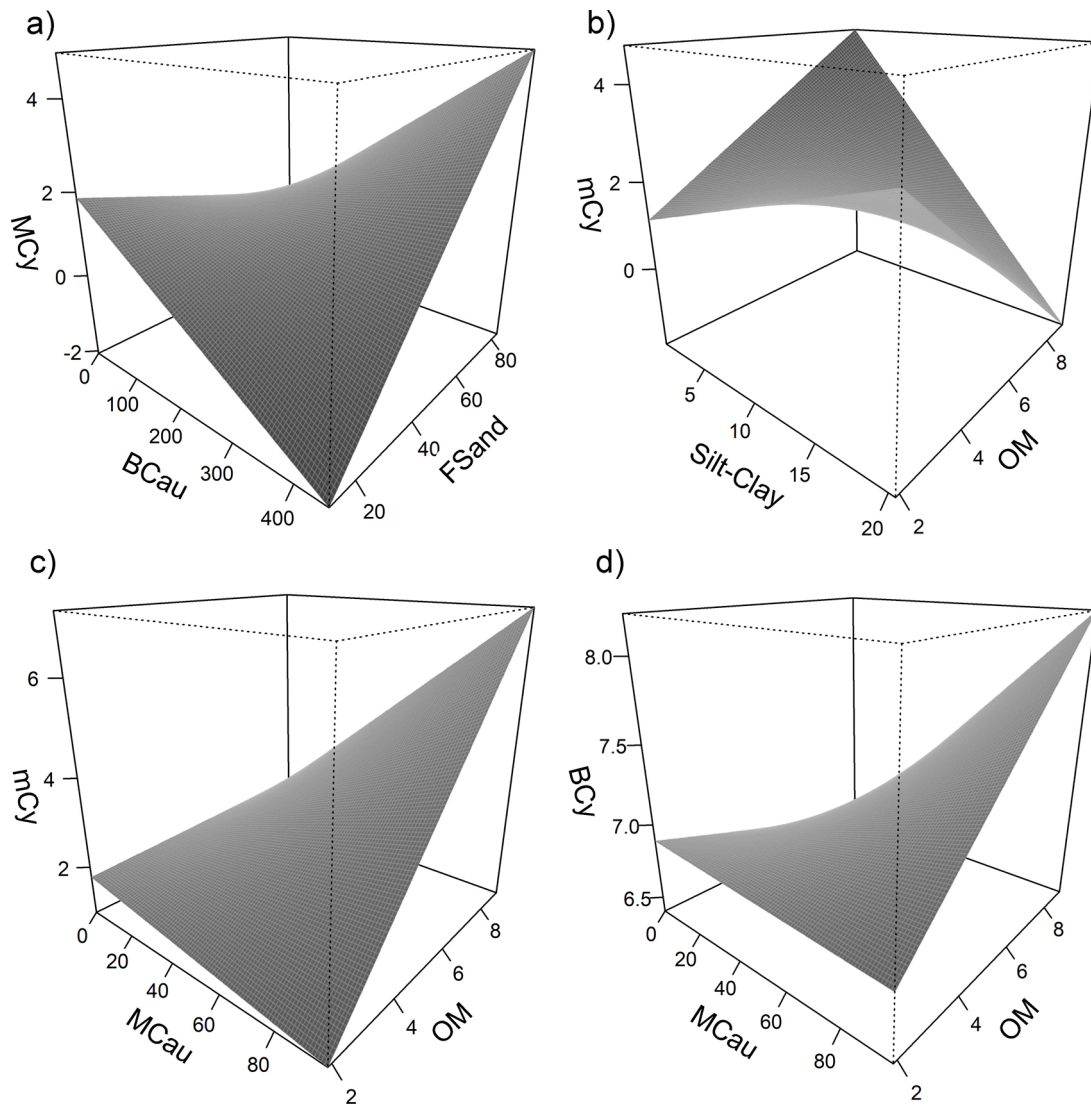


Fig. 5. Graphical representations of the significant coefficients fitted in the *C. nodosa* shallow bottom models. a) Interactive effect of *C. prolifera* biomass (BCau) and fine sand (FSand) on *C. nodosa* macrocover (MCy), b) effect of the interaction of Silt-Clay and organic matter (OM) on *C. nodosa* mesocover (mCy), c-d) effect of the interaction of *C. prolifera* macrocover (MCau) and OM on mCy and *C. nodosa* shoot density (DCy).

variation in seagrass mesocover in the lagoon. Further experimental studies would be necessary to fully understand the complex relationships between the two macrophytes at this level. In any case, since both macrophytes had concomitantly shown greater abundances and biomasses on sediments with the highest OM content, and that this pattern was consistent on deep and shallow bottoms, the assumption that *C. prolifera* negatively influences, directly or indirectly, *C. nodosa* distribution in the Mar Menor can be rejected.

The distribution of macrophytes in the Mar Menor in 2014 was similar to a previous map from the early 1980s (Fig. S7), just a few years after the introduction and spread of *C. prolifera* in the ecosystem, and contrasts with subsequent estimations conducted in 2003 and 2008 (Lloret et al., 2005; Pérez-Ruzafa et al., 2012). These latter studies reported the presence of *C. nodosa* in just a few shallow areas of the lagoon and suggested that *C. prolifera* had almost completely substituted the seagrass along the length of the whole lagoon between the 1980s and 2000s. We found it unlikely, however, that *C. nodosa* had recolonised most of the lagoon between 2008 (date of the last map; Pérez-Ruzafa et al., 2012) and 2014 (this study) from just a few small relict populations and without any substantial improvement in quality of the lagoon water. In fact, the species needed almost one decade to partially

recolonise (estimated 40 % recovery) a much smaller Mediterranean coastal lagoon after water quality improvement (Garrido et al., 2013). This means that even with improved water quality, recolonisation by *C. nodosa* of large areas of the Mar Menor would take much longer than only a few years. Alternatively, and most likely, the inconsistency noted between our vegetation map and those from the preceding decade could have resulted from methodological aspects related to sampling and mapping and to the spatial resolution of the studies required to integrate the heterogeneity of both the lagoon and the seagrass population structure at different spatial scales.

In conclusion, the distribution of the seagrass *C. nodosa* in the Mar Menor in 2014 did not seem to have undergone drastic changes since the invasion and rapid spread of the seaweed *C. prolifera* four decades before. Both species coexisted in the lagoon during this period and were the dominant macrophytes over the entire lagoon seabed at the time this study was conducted, with abundance patterns that mainly reflected their specific ecological requirements (e.g., light conditions); albeit the influence of human pressures and coastal works may have had a strong influence in the shallower areas of the lagoon. The seagrass was found thriving intermingled with dense *C. prolifera* beds on highly anoxic muddy sediments over large areas of the lagoon floor, which, together

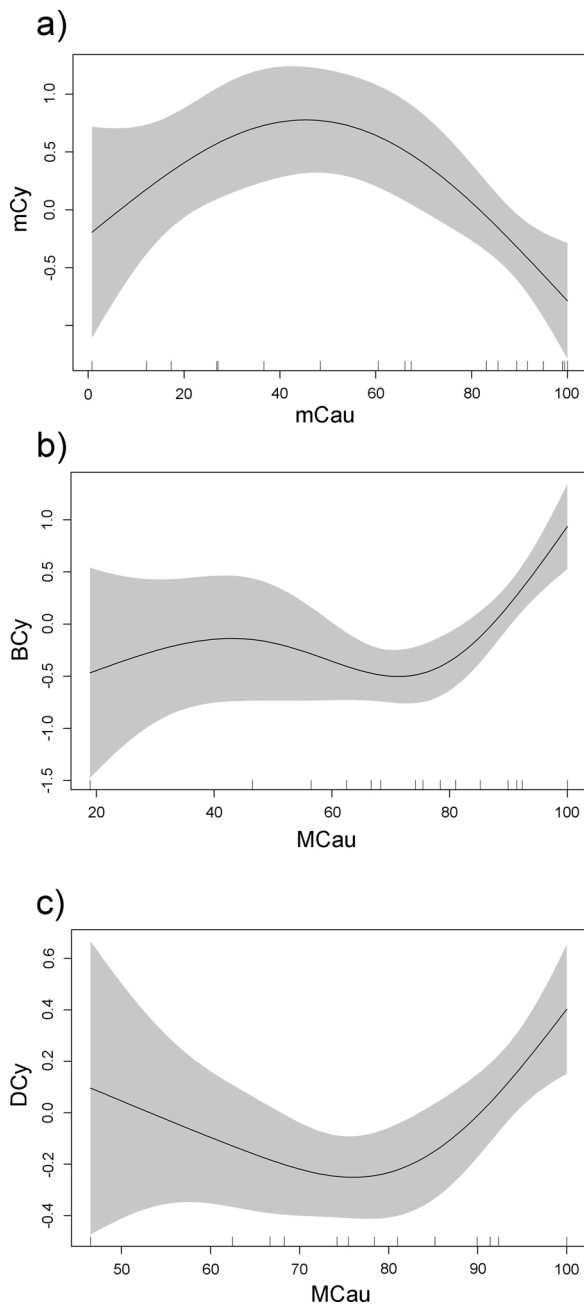


Fig. 6. Smoothing spline relationships between *C. nodosa* and *C. prolifera* abundance derived from GAMs analysis of the deep bottoms. Variables: *C. nodosa* mesocover (mCy), biomass (BCy) and shoot density (DCy), and *C. prolifera* mesocover (mCau) and macrocover (MCau).

with findings derived from models, did not support a negative direct or indirect influence of *C. prolifera* on *C. nodosa* in this ecosystem. On the basis of the above, we can confirm that *C. prolifera* was not progressively replacing *C. nodosa* in the lagoon. However, increasing human pressures and ongoing climate change could upset this balance, substantially changing the abundance and distribution of these macrophytes and thus lessening the overall resilience of the ecosystem to future environmental pressures.

Author contributions

BMD, JB-E, JMR and PG: study design, methodology and field sampling. MDB and RG-M: field sampling and laboratory analyses. MDB, JB-

E and IP: statistical analyses. MDB and AR-S: mapping and ArcGIS analyses. MDB, LM-G and JMR: writing the original draft, reviewing and editing. All the authors critically contributed to the drafts and gave final approval for publication.

Declaration of Competing Interest

The authors declare no competing interest.

Acknowledgments

This work was supported by Projects G30072540 and FBCC2017 co-funded by the Spanish NGO *Asociación de Naturalistas del Sureste* and the Biodiversity Foundation of the Spanish Ministry of Ecological Transition and Demographic Challenge, and by Spanish Project UMBRAL (*Responses of marine benthic macrophytes to stress: critical transitions, resilience and management opportunities*) financed by the National Plan of Research of the Spanish Government (CTM2017-86695-C3-2-R). The work was also supported by the DMEMM project financed by the Spanish Oceanography Institute. M.B.D. and J.B.E were supported by a contract within the program Personal Técnico de Apoyo funded by the Ministry of Science and Innovation. The authors wish to thank training students Judit Jiménez Casero, Manuel Rosendo Conde Caño, Irene Nadal Arizo, Ángela Ángel Moreno Briones, Jean Ibagnes and Norma María López Rosique for their help during field samplings and for assisting with laboratory measurements. We acknowledge logistical support provided by President and Staff of the harbours Club Nautico Lo Pagán, Club Náutico La Puntica and Centro de Actividades Náuticas (San Pedro del Pinatar, Murcia, Spain). We thank Regional Government of Murcia (Consejería de Agricultura, Agua y Medio Ambiente), and national authorities (MITECO) for permission.

Appendix A. Supplementary data

Supplementary material related to this article can be found, in the online version, at doi:<https://doi.org/10.1016/j.aquabot.2021.103415>.

References

- Alexandre, A., Baeta, A., Engelen, A.H., Santos, R., 2017. Interactions between seagrasses and seaweeds during surge nitrogen acquisition determine interspecific competition. *Sci. Rep.* 7, 1–8. <https://doi.org/10.1038/s41598-017-13962-4>. Springer US.
- Ballester, R., 1985. Biomasa, estacionalidad y distribución de tres macrofitos: *Ruppia cirrhosa*, *Cymodocea nodosa* y *Caulerpa prolifera* en el Mar Menor (Murcia, SE de España). *Anales de Biología* 31–36.
- Bernardeau-Esteller, J., Ruiz, J.M., Tomas, F., Sandoval-Gil, J.M., Marín-Guirao, L., 2015. Photoacclimation of *Caulerpa cylindracea*: light as a limiting factor in the invasion of native Mediterranean seagrass meadows. *J. Exp. Mar. Biol. Ecol.* 465, 130–141. <https://doi.org/10.1016/j.jembe.2014.11.012>.
- Bernardeau-Esteller, J., Marín-Guirao, L., Sandoval-Gil, J.M., García-Muñoz, R., Ramos-Segura, A., J.M. Ruiz., 2020. Evidence for the long-term resistance of *Posidonia oceanica* meadows to *Caulerpa cylindracea* invasion. *Aquat. Bot.* 160, 103–167. <https://doi.org/10.1016/j.aquabot.2019.103167>.
- Burkpile, D.E., Hay, M.E., 2006. Herbivore vs. nutrient control of marine primary producers: Context-dependent effects. *Ecology* 87, 3128–3139. [https://doi.org/10.1890/0012-9658\(2006\)87\[3128:HVNCOM\]2.0.CO;2](https://doi.org/10.1890/0012-9658(2006)87[3128:HVNCOM]2.0.CO;2).
- Ceccherelli, G., Cinelli, F., 1997. Short-term effects of nutrient enrichment of the sediment and interactions between the seagrass *Cymodocea nodosa* and the introduced green alga *Caulerpa taxifolia* in a Mediterranean bay. *J. Exp. Mar. Biol. Ecol.* 217, 165–177. [https://doi.org/10.1016/S0022-0981\(97\)00050-6](https://doi.org/10.1016/S0022-0981(97)00050-6).
- Ceccherelli, G., Sechi, N., 2002. Nutrient availability in the sediment and the reciprocal effects between the native seagrass *Cymodocea nodosa* and the introduced rhizophytic alga *Caulerpa taxifolia*. *Hydrobiologia* 474, 57–66. <https://doi.org/10.1023/A:1016514621586>.
- Collier, C.J., Lavery, P.S., Ralph, P.J., Masini, R.J., 2008. Physiological characteristics of the seagrass *Posidonia sinuosa* along a depth-related gradient of light availability. *Mar. Ecol. Prog. Ser.* 353, 65–79. <https://doi.org/10.3354/meps07171>.
- Conesa, H.M., Jiménez-Cárceles, F.J., 2007. The Mar Menor lagoon (SE Spain): a singular natural ecosystem threatened by human activities. *Mar. Pollut. Bull.* 54, 839–849. <https://doi.org/10.1016/j.marpolbul.2007.05.007>.
- Costanza, R., de Groot, R., Farberll, S., Grassot, M., Hannon, B., Limburg, K., Naeem, S., et al., 1997. The value of the world's ecosystem services and natural capital. *Nature* 253–260.

- Terrados, J., 1991. Crecimiento y producción de las praderas de macrófitos del Mar Menor, Murcia. Ph.D. Thesis. Universidad de Murcia, España.
- Terrados, J., Ros, J., 1991. Production dynamics in a macrophyte-dominated ecosystem: the Mar Menor coastal lagoon (SE Spain). *Oecologia Aquatica* 10, 255–270.
- Terrados, J., Ros, J., 1992. Growth and primary production of *Cymodocea nodosa* (Ucria) Ascherson in a Mediterranean coastal lagoon: the Mar Menor (SE Spain). *Aquat. Bot.* 43, 63–74. [https://doi.org/10.1016/0304-3770\(92\)90014-A](https://doi.org/10.1016/0304-3770(92)90014-A).
- Terrados, J., Duarte, C.M., Kamp-Nielsen, L., Agawin, N.S.R., Gacia, E., Lacap, D., Fortes, M.D., Borum, J., Lubanski, M., Greve, T., 1999. Are seagrass growth and survival constrained by the reducing conditions of the sediment? *Aquat. Bot.* 65, 175–197. [https://doi.org/10.1016/S0304-3770\(99\)00039-X](https://doi.org/10.1016/S0304-3770(99)00039-X).
- Thomsen, M.S., Wernberg, T., Engelen, A.H., Tuya, F., Vanderklift, M.A., Holmer, M., McGlathery, K., Arenas, F., Kotta, J., Silliman, B.R., 2012. A meta-analysis of seaweed impacts on seagrasses: generalities and knowledge gaps. *PLoS One* 1. <https://doi.org/10.1371/journal.pone.0028595>.
- Tuya, F., Hernandez-Zerpa, H., Espino, F., Haroun, 2013. Drastic decadal decline of the seagrass *Cymodocea nodosa* at Gran Canaria (eastern Atlantic): interactions with the green algae *Caulerpa prolifera*. *Aquat. Bot.* 105, 1–6. <https://doi.org/10.1016/j.aquabot.2012.10.006>.
- Valiela, I., McClelland, J., Hauxwell, J., Behr, P.J., Hersh, D., Foreman, K., 1997. Macroalgal blooms in shallow estuaries: controls and ecophysiological and ecosystem consequences. *Limnol. Oceanogr.* 42, 1105–1118. <https://doi.org/10.4319/lo.1997.42.5.part.2.1105>.
- Velasco, J., Lloret, J., Millan, A., Marin, A., Barahona, J., Abellan, P., Sanchez-Fernandez, D., 2006. Nutrient and particulate inputs into the Mar Menor lagoon (SE Spain) from an intensive agricultural watershed. *Water Air Soil Pollut.* 176, 37–56. <https://doi.org/10.1007/s11270-006-2859-8>.
- Vidondo, B., Duarte, C.M., Middelboe, A.L., Stefansen, K., Lützen, T., Nielsen, S.L., 1997. Dynamics of a landscape mosaic: size and age distributions, growth and demography of seagrass *Cymodocea nodosa* patches. *Mar. Ecol. Prog. Ser.* 158, 131–138. <https://doi.org/10.3354/meps158131>.
- Williams, S.L., Grosholz, E.D., 2002. Preliminary reports from the *Caulerpa taxifolia* invasion in southern California. *Mar. Ecol. Prog. Ser.* 233, 307–310. <https://doi.org/10.3354/meps233307>.
- Williams, S.L., Smith, J.E., 2007. A global review of the distribution, taxonomy, and impacts of introduced seaweeds. *Annu. Rev. Ecol. Evol. Syst.* 38, 327–359. <https://doi.org/10.1146/annurev.ecolsys.38.091206.095543>.